How to cite: *Angew. Chem. Int. Ed.* **2024**, *63*, e202317844
doi.org/10.1002/anie.202317844

Electrocatalysis

Electrocatalytic Transfer Hydrogenation of 1-Octene with [(^{tBu}PCP)Ir(H)(Cl)] and Water

*Patrick Mollik, Markus Drees, Alexander M. Frantz, and Dominik P. Halter**

Abstract: Electrocatalytic hydrogenation of 1-octene as non-activated model substrate with neutral water as H-donor is reported, using [(^{tBu}PCP)Ir(H)(Cl)] (**1**) as the catalyst, to form octane with high faradaic efficiency (FE) of 96 % and a k_{obs} of 87 s^{-1}. Cyclic voltammetry with **1** revealed that two subsequent reductions trigger the elimination of Cl^- and afford the highly reactive anionic Ir(I) hydride complex [(^{tBu}PCP)Ir(H)]$^-$ (**2**), a previously merely proposed intermediate for which we now report first experimental data by mass spectrometry. In absence of alkene, the stoichiometric electrolysis of **1** in THF with water selectively affords the Ir(III) dihydride complex [(^{tBu}PCP)Ir(H_2)] (**3**) in 88 % FE from the reaction of **2** with H_2O. Complex **3** then hydrogenates the alkene in classical fashion. The presented electro-hydrogenation works with extremely high FE, because the iridium hydrides are water stable, which prevents H_2 formation. Even in strongly alkaline conditions (Bu_4NOH added), the electro-hydrogenation of 1-octene with **1** also proceeds cleanly (89 % FE), suggesting a highly robust process that may rely on H_2O activation, reminiscent to transfer hydrogenation pathways, instead of classical H^+ reduction. DFT calculations confirmed oxidative addition of H_2O as a key step in this context.

Introduction

Hydrogenation of organic molecules is a process of paramount importance for the synthesis of base- and fine chemicals, pharmaceutically active compounds, and energy carriers, as well as for biomass valorization, both on industrial and laboratory scale.[1–7] To avoid challenges of handling gaseous H_2 at high temperatures and pressures necessary for chemical hydrogenation (CH), transfer hydrogenation (TH) has matured as a powerful alternative.[1,8,9] TH employs chemical H-donors such as predominantly used isopropanol or formic acid as a substitute for H_2. In both cases of CH and TH, the reduction equivalents for the net reduction of substrates during hydrogenation are provided by H_2 or the H-donor as chemical reducing agents.

For increased atom economy and cost efficiency, it would be desirable to enable H_2O as a cheap and abundant H-donor for TH instead of isopropanol or formate.[10] However, H_2O cannot provide the necessary reduction equivalents, which is why existing examples of hydrogenation with H_2O depend on the use of external reducing agents including Zn powder,[10–12] In powder,[13] or bis(pinacolato)diboron.[14,15] Electrochemistry can be an elegant substitute for such sacrificial electron donors, which has led to a third branch of hydrogenation catalysis, namely electrocatalytic hydrogenation (ECH). Remarkable examples of ECH have been reported for the conversion of alkenes to alkanes,[16,17] selective semi-hydrogenation of alkynes to alkenes,[18–20] exhaustive hydrogenation of arenes,[21–23] selective hydrogenation of arenes to 1,4-dienes,[24] hydrogenation of organic carbonyls,[25–27] or the deoxygenation of biomass.[28–30] ECH has even proven to be a powerful method for the synthesis of selectively deuterated alkenes.[31] Both, noble metal electrodes and molecular catalysts are employed for these conversions.[32] The dominant common aspect of all these examples is that they rely on H^+ reduction, often in highly acidic electrolyte. The working principle is to either generate H_2 or surface hydrides in situ at the electrode for immediate consumption by a coupled hydrogenation reaction.[33] Examples of molecular ECH catalysts likewise operate by formation of reactive metal-hydride species via H^+ reduction, with a remarkable exception by Peters and co-workers, who elegantly separated redox reactive metal center and proton acceptor site in their anilinium cobaltocene catalyst.[26,34,35] While these existing systems succeed at avoiding external H_2 gas feeds or sacrificial electron donors for hydrogenation, several drawbacks impede application. In many cases faradaic efficiencies for hydrogenated products are low, given that H_2 evolution (HER) remains the dominant process.[36] Also poor solubility of most relevant organic substrates in acidic aqueous electrolytes requires less convenient emulsion electrolysis with the use of surfactants.[37,38] The requirement of high proton activity may interfere with functional groups of substrates that cannot tolerate low pH, and the harsh conditions of acidic electrolyte can lead to side reactions. Exemplarily, for ECH of toluene to methylcyclohexane on Pt electrodes in acid electrolyte, side reactions as severe as

[*] P. Mollik, Dr. M. Drees, A. M. Frantz, Dr. D. P. Halter
Technical University of Munich, TUM School of Natural Sciences, Department of Chemistry, Chair of Inorganic and Metal-Organic Chemistry, Lichtenbergstr. 4, 85748 Garching, Germany
E-mail: dominik.halter@tum.de

C–C bond cleavage to yield CH_4 and cyclohexane were observed.[37] Finally and importantly, with H_2O oxidation (OER) at the counter electrode, low pH electrolytes cause high overpotentials, catalyst degradation, and sluggish kinetics of the coupled oxidation reaction.[39] This generates a high cell potential and limits overall achievable process efficiencies. For the multitude of these reasons, it would be desirable to establish ECH reactions that proceed in organic electrolyte with neutral pH water, or even in alkaline media, instead of under acidic conditions.

Drawing from extensive literature on TH,[1,8] and inspired by examples that show metal-hydrides can also be formed by oxidative addition of H_2O to low-valent transition metal complexes instead of by H^+ reduction,[40] we hypothesized that a pathway independent of acidic protons should be accessible for electrocatalytic transfer hydrogenation (e-TH) with water as the formal H-donor and electrons as the reducing agent.

[($^{t\text{Bu}}$PCP)Ir(H)(Cl)] (**1**) was chosen as a model catalyst for our proof of principle study, since it is known to mediate alkene hydrogenation with water tolerant hydride intermediates, does not decompose in water, and its Ir(I) derivative complex [($^{t\text{Bu}}$PCP)Ir] oxidatively adds H_2O to afford a stable hydroxo-hydrido species.[41]

Electro-hydrogenation with H_2O is generally rarely demonstrated for molecular electrocatalysts, since the proton sources used typically need a sufficiently acidic pKa value to enable catalysis. Particularly for heterogeneous hydrogenation, however, there are inspiring examples that operate with water,[42] even under strong alkaline conditions.[43,44]

We investigated the electrochemically accessible redox reactivity of the Ir(III) pincer complex **1** and studied its electrochemically triggered chemical reactions with water and 1-octene as an unactivated model alkene. The e-TH activity of **1** was confirmed by octane production with quantitative faradaic efficiency (FE). We generally assessed the proton activity dependence of the observed electro-hydrogenation by adding the strong base tetrabutylammonium hydroxide (Bu_4NOH) to the electrolysis solution, and found that *n*-octane was still produced with great FE of 89 %, suggesting that H_2O activation rather than H^+ reduction may drive catalysis. Mechanistic studies and stoichiometric control reactions revealed that the e-TH at room temperature involves an electro-generated anionic Ir(I) hydride complex as the key reactive species that activates H_2O. The combined results suggest that the iridium hydride is regenerated by oxidative addition of water in reminiscence of classical transfer hydrogenation. This represents a major difference compared to existing electro-hydrogenation catalysts that are principally driven by in situ proton reduction, and may inspire the general further development of such e-TH reactivity.

Results and Discussion

[($^{t\text{Bu}}$PCP)Ir(H)(Cl)] (**1**, with $^{t\text{Bu}}$PCP–H = 1,3-bis((di-*tert*-butylphosphino)methyl)benzene) was synthesized according to literature procedures,[45,46] and studied by cyclic voltammetry (CV) to elucidate its e-TH reactivity. At first, a CV of **1** was recorded in organic electrolyte (0.3 M Bu_4NPF_6 (tetrabutylammonium hexafluorophosphate) in THF, all potentials referenced *vs.* Fc^+/Fc) to reveal fundamental redox reactivity of the complex (Figure 1, left). In the examined potential window between +0.3 and −3.3 V (SI, Figure S3), **1** features an irreversible reduction at a peak potential of −2.55 V, and a second reduction event at a half wave potential of −2.84 V, which shows quasi-reversibility at scan rates above 0.1 V/s (Figure 1, left). The reduction events are assigned to Ir(III)/Ir(II) and Ir(II)/Ir(I) couples, respectively, with a detailed characterization presented in the mechanistic considerations section (see below).

The electrochemical accessibility of an Ir(I) species in ($^{t\text{Bu}}$PCP)$^-$ environment sets the stage to investigate the proposed e-TH with water. Encouragingly, addition of 1-octene and water as the H-donor to the electrolyte containing complex **1**, indeed yielded a catalytic current enhancement that is visibly tied to the Ir(II)/Ir(I) reduction potential (Figure 1, right). Control experiments with either of the three components alkene, H_2O or catalyst missing did not yield a comparable catalytic current response (*c.f.* mechanistic considerations section). Bulk electrolysis experiments performed at −3.3 V *vs.* Fc^+/Fc in the presence of 1-octene, H_2O, and catalyst precursor **1** produced *n*-octane as the hydrogenated product at high faradaic efficiency of 96 % with a TON of 22, based on GC-FID analysis of the electrolyte solution after electrolysis (SI, Section 5.1). An observed rate constant k_{obs} of 87 s^{-1} was determined for the hydrogenation of 1-octene with **1**, based on foot-of-the-wave analysis, (SI, Section 4). The high FE, which we consider quantitative in view of the work up by vacuum distillation, and therefore the desirable lack of competing H_2 evolution is likely due to the literature known water stability of iridium hydrides.[41,47,48] Principally, the catalyst can be reused for a subsequent run by adding fresh THF solvent as well as new 1-octene and H_2O substrates to the solid catalyst

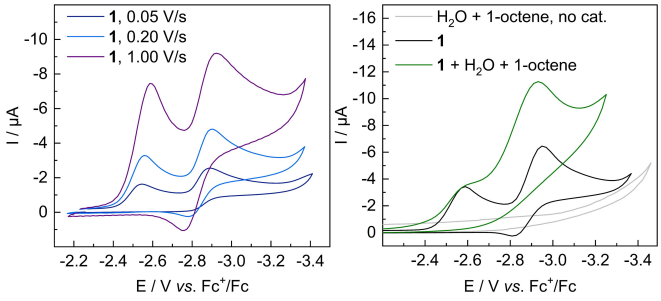

Figure 1. CV data, recorded using a GC disc (1 mm) working electrode, a Pt wire counter electrode, and a silver wire pseudo reference electrode with ferrocene added for referencing. Left: CV of **1** (2 mg) in THF with Bu_4NPF_6 (0.3 M, 3 mL) recorded at different scan rates. Right: CV of **1** (3 mg) in THF with Bu_4NPF_6 (0.1 M, 5 mL) recorded at a scan rate of 0.2 V/s. The green trace shows the catalytic current response after addition of 100 µL degassed H_2O and 50 µL 1-octene. The grey trace shows the CV response of the identical electrolyte solution with H_2O and 1-octene, but in absence of catalyst **1**.

and electrolyte salt residue after product separation by vacuum transfer (SI, Section 5.6.). Also, a scale-up perspective of the electro-hydrogenation reaction was investigated, increasing the space-time-yield by 2 orders of magnitude with high surface area carbon fiber working electrodes (SI, Section 5.7).

Importantly, in the absence of catalyst **1**, no *n*-octane was formed by electrolysis under otherwise identical conditions as confirmed by a control experiment (SI, Section 5.4). Together, the high activity and faradaic efficiency confirmed the excellent performance of catalyst **1** for electro-hydrogenation, which prompted us to further investigate the underlying catalytic reactivity.

Mechanistic Considerations

Starting from **1** as the catalyst precursor, the first step towards e-TH is the conversion of **1** into its active form by electrochemical reduction, as evidenced by the fact that catalytic electro-hydrogenation current is tied to the Ir(II)/Ir(I) reduction potential. Scan rate dependent CV (Figure 1, left) show that the first reduction of **1** remains irreversible even at high scan rate of 1 V/s; thus, suggesting a fast chemical reaction is triggered by this reduction. The most likely hypothesis is that Ir(III)/Ir(II) reduction generates a fleeting anionic Ir(II) complex, which instantly seeks charge neutrality by eliminating a Cl^- ligand to yield the proposed intermediate Ir(II) species as described in Scheme 1. This hypothesis is supported by the fact that the addition of excess chloride ions to the electrolyte renders the reduction peak at −2.55 V also quasi reversible at high scan rates (SI, Figure S4). The reason is that Cl^- dissociation from the reduced Ir complex is hampered (or re-coordination of Cl^- is favored) in media with high chloride activity. Furthermore, DFT calculations suggest that the 15 valence electron (VE) complex [($^{t\text{Bu}}$PCP)Ir(H)] formed after Cl^- elimination is then stabilized by coordination of an L-type ligand (THF or H_2O) to afford a 17 VE species.

The second reduction event at −2.84 V reduces the proposed 17 VE Ir(II) intermediate by another electron, to yield an Ir(I) species. At scan rates below 0.1 V/s, this reduction event is also irreversible, likely because of the well-known high reactivity of Ir(I) complexes that even activate C–H bonds of alkanes.[49] However, the fact that at higher scan rates the second reduction event becomes more and more reversible (Figure 1, left), strongly suggests that the Ir(I) complex formed remains an anionic species [($^{t\text{Bu}}$PCP)Ir(H)]$^-$ (**2**) that does not lose its hydride ligand. In fact, based on quantum chemical calculations by Ahlquist et al. an anionic hydride species related to **2**, but in a ($^{t\text{Bu}}$POCOP)$^-$ pincer ligand environment, was previously proposed as the active species for electrochemical CO_2 reduction to formate with the POCOP analogue of complex **1**.[50,51] With our own quantum chemical calculations (SI, section 8), we analyzed reduction potentials of our experimental reduction cascade following procedures by Grimme and co-workers,[52] which predict a reduction potential of only −1.86 V to convert a hypothetical 15 VE Ir(II) species [($^{t\text{Bu}}$PCP)Ir(H)] to anionic Ir(I) complex **2**. Coordination of an L-type ligand (L = THF or H_2O in our case) to the 15 VE complex affords the much more stable 17 VE complex [($^{t\text{Bu}}$PCP)Ir(H)(L)], for which a Ir(II)/Ir(I) reduction potential of −3.1 V was calculated, which is—in view of achievable accuracy of such calculations—in good agreement with our experimentally determined value of −2.84 V for the Ir(II)/Ir(I) couple.

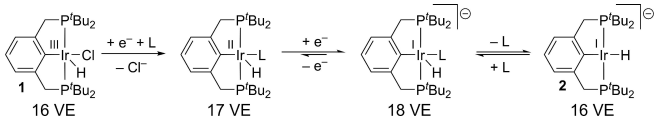

Scheme 1. Proposed underlying reactivity of the two consecutive electrochemical reduction events observed for complex **1**.

Further confirmation for the existence of the anionic Ir(I) hydride **2** as the final product of the overall two-electron reduction was obtained from negative mode LIFDI-MS (liquid injection field desorption ionization mass spectrometry) control experiments. For this, **1** was in situ reduced chemically by treatment with a solution of solvated electrons (electride [K^+(2.2.2-cryptand)][e^-(solv.)]) in THF at low temperature in lieu of electrochemically provided electrons (SI, section 2.2. for details),[53] and injected into the LIFDI-MS immediately. A prominent molecular ion peak at 587.2562 m/z (theoretically 587.2553 m/z) with the expected isotope pattern of anionic hydride complex **2** was measured (SI, Figure S32); thus, providing first experimental evidence for the existence of such previously only theoretically proposed anionic Ir(I) hydrides. Accordingly, the electrochemical response of **1** as presented in Figure 1 (left) is interpreted as shown in Scheme 1.

Entering the electrocatalytic cycle for e-TH with electro-activated complex **2**, opens up a variety of plausible reaction pathways, which will be discussed and evaluated in the following. Based on the combined electrochemical results, our control experiments, and literature support including a quantum chemical evaluation published for CO_2 reduction on the related POCOP system,[48,50,54] the reaction cascade shown in Scheme 2 is proposed as a likely mode of operation for the electro-hydrogenation of alkenes with **1**.

Considering the high affinity of iridium complexes for alkenes, a first mechanistic consideration was, whether under catalytic conditions precursor complex **1** would be coordinated by an alkene even prior to its electrochemical activation. This possibility was excluded by DOSY NMR experiments, in which no alkene coordination to the complex was observed (SI, Figure S39). We like to note that for all ^{1}H NMR control experiments styrene was used as a model alkene, due to its more reliably interpretable NMR features compared to 1-octene (SI, Section 6.2). Also no reactivity of **1** towards styrene, as even more reactive alkene than 1-octene, was observed in the presence of water according to NMR control experiments (SI, Figure S40). Additionally, the electrochemical reduction potential of complex **1** does not shift in presence of 1-octene (Figure 2, Left), which would be expected for coordination of an extra

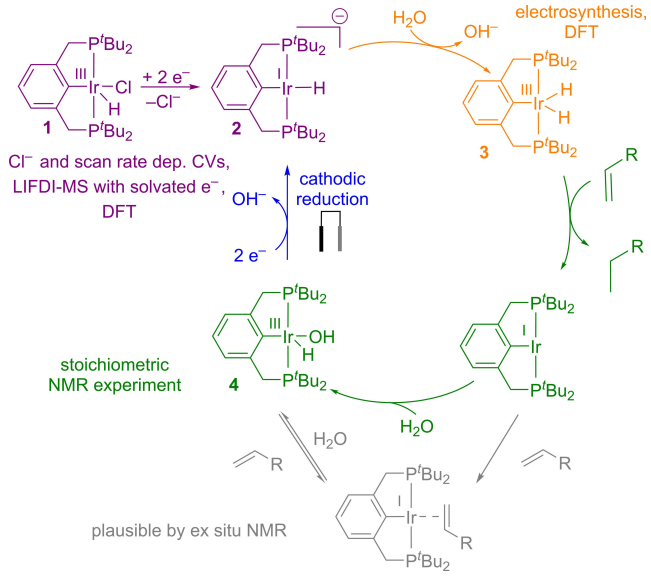

Scheme 2. Proposed reaction cascade for electrocatalytic hydrogenation of alkenes with water at catalyst **1**, color coded and labeled with methods of experimental support for each reaction step.

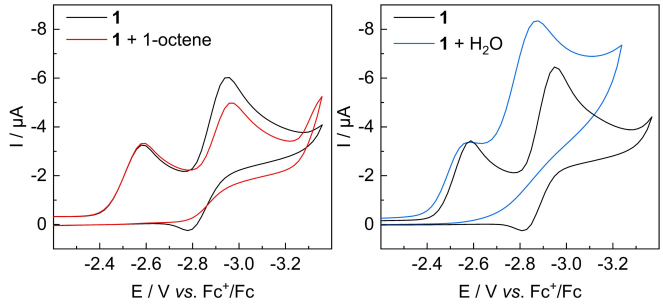

Figure 2. CV data, recorded at a scan rate of 0.2 V/s in THF with Bu_4NPF_6 (0.1 M, 5 mL) using a GC disc (1 mm) working electrode, and a Pt wire counter electrode. Left: Current responses of complex **1** (3 mg) before (black trace) and after addition of 50 µL 1-octene (red trace) in anhydrous electrolyte. Data was measured against a leakless Ag/AgCl reference electrode compatible with organic electrolyte and referenced by addition of ferrocene. Right: Current responses of complex **1** (3 mg) before (black trace) and after addition of 100 µL H_2O (blue trace). Data was measured against a Ag wire pseudo reference electrode and referenced by addition of ferrocene.

π-acceptor ligand. Hence, the most plausible scenario is that electro-generated species **2** enters the e-TH reaction cycle.

Under catalytic conditions, **2** may then either react with an alkene to form an anionic Ir(I) alkyl species in analogy to quantum chemical calculations for CO_2 insertion,[48,50] or **2** could react with H_2O to yield charge neutral Ir(III) dihydride complex [($^{t\text{Bu}}$PCP)Ir(H_2)] (**3**) under elimination of OH^-. For the alkene first pathway, we refer again to the data plotted in Figure 2, where upon addition of 1-octene, the second reduction event loses reversibility and shows slightly reduced peak current. In principle, the decreased peak current of the second reduction could be attributed to a slow chemical reaction between the singly reduced Ir-complex and the alkene. Additionally, the complete irreversibility of the second reduction event in the presence of 1-octene could point to a reaction of anionic hydride **2** with the alkene. However, we like to emphasize that such EC reaction cascades induce a rate constant dependent shift of the reduction peaks to less negative potentials.[55] Since such a signal shift is not observed to an appreciable extent, the aforementioned reactions can only be very slow, which then should not represent a main pathway of catalysis.

In turn, CV experiments with **1** and H_2O in the absence of an alkene substrate, show an unchanged first reduction event together with a fully irreversible second reduction peak that is shifted to less negative potential by 70 mV; thus, indicating a fast reaction with H_2O.

We have investigated this reaction further, by conducting controlled potential electrolysis at −3.3 V (the same potential as under catalytic hydrogenation) in an H-cell charged with complex **1** and H_2O and observed the formation of Ir(III) dihydride complex **3** with 88 % FE according to ^{31}P NMR spectroscopy (SI, Section 2.6. and Figure S38). This finding confirms the proposed reaction of electro-generated **2** with H_2O as shown in the orange section of Scheme 2.

Having identified the reaction product of electro-generated **2** and H_2O to be complex **3**, we have also characterized a chemically synthesized sample of **3** by CV (SI, Figure S5), and observed a reversible reduction event at a half-wave potential of −2.85 V. This finding nicely explains the enhanced peak current in the right section of Figure 2, by revealing an ECE mechanism, in which **2** is produced (E_1) and reacts with H_2O to form **3** (C), upon which Ir(III) complex **3** is reduced again (E_2).

Therefore, under catalytic conditions either electro-generated **3** or also its electro-reduced form can react with 1-octene. For **3**, the reaction follows the classical established pathway for hydrogenation of non-polar substrates by redox reactive metal catalysts,[1] which yields the Ir(I) complex [($^{t\text{Bu}}$PCP)Ir] as the next plausible intermediate. While [($^{t\text{Bu}}$PCP)Ir] is a well-accepted intermediate in many literature reports,[41,56–58] it is too reactive to be isolated. In the presence of H_2O, however, [($^{t\text{Bu}}$PCP)Ir] is known to be trapped quantitatively in form of [($^{t\text{Bu}}$PCP)Ir(H)(OH)] (**4**) formed by oxidative addition of water,[41] which replenishes the metal-hydride functionality for the catalytic cycle. Despite literature precedent for this reactivity, presented as green section in Scheme 2, we experimentally confirmed the relevance of this reaction cascade under our catalytic conditions, by synthesizing **3** and reacting it with styrene (as a more ^{1}H NMR characteristic substrate than *n*-octene) and water in THF-d_8 for NMR spectroscopic analysis. As expected, ethylbenzene and complex **4** were obtained (SI, Figure S41 and S42).

Considering the OH^- ligand in **4** a pseudo halogen highlights the chemical similarity between complex **1**—the catalyst precursor—and complex **4** the terminal product of the electro-hydrogenation cascade. Accordingly, the final step that closes the catalytic cycle (blue section in Scheme 2) is the two-electron reduction of complex **4** to liberate OH^- under regeneration of active species **2**. This final reaction step was confirmed by chemical synthesis of complex **4**, which in CV analysis showed a reduction at a peak potential

of −3.00 V, comparable to complex **1**. Expectedly, the two one-electron reduction events of complex **4** overlap (SI, Figure S6), due to a redox potential shift caused by different Lever Parameters of OH^- and Cl^-.[59] Additionally, when using complex **4** as the catalyst precursor instead of **1**, identical e-TH performance was observed to likewise generate *n*-octane with 97 % FE (SI, Section 5.2); thus, establishing that **4** can actively participate in the catalytic cycle as proposed in Scheme 2.

While the above described reaction steps build an electrocatalytic cycle for which we have experimental support, further parallel reactivity seems plausible, which will be discussed in the following. Most importantly, the electro-activated species **2** may first react with 1-octene instead of with water, as proposed for catalytic CO_2 reduction.[48,50] CV measurements as presented in Figure 2, Left suggest plausibility but relatively slow kinetics for this pathway to be competitive to the H_2O-first pathway. Nevertheless, given that the faradaic efficiency of 1-octene hydrogenation under electrocatalytic conditions is quantitative, we conclude that either in the presence of water the reaction of **2** with the alkene is kinetically outcompeted, also favored by a much higher concentration and diffusion coefficient of water with respect to the alkene, or that in presence of water the reaction product of **2** and 1-octene is successfully converted into the alkane and an iridium complex that can be part of the active electrocatalytic cycle.

A further aspect of our mechanistic considerations targets off-cycle intermediates that are in equilibrium with our proposed cycle. Specifically, reactive intermediate [($^{t\text{Bu}}$PCP)Ir] may be stabilized by coordination of alkenes as off-cycle species that we cannot detect under catalytic conditions, although their formation seems likely and is supported by quantum chemical calculations.[57,60] Based on established reaction equilibria between [($^{t\text{Bu}}$PCP)Ir], alkene complexes like the literature known styrene adduct [($^{t\text{Bu}}$PCP)Ir(CH_2=CH–Ph)] and [($^{t\text{Bu}}$PCP)Ir(H)(OH)], it is clear that such an alkene adduct would straightforwardly be converted back into the hydroxo-hydrido species **4** of the active cycle by reaction with water.[41,60] ^{1}H NMR control reactions (SI, Figure S29) confirm this equilibrium for our specific compounds. Accordingly, the full interplay of chemical reaction sequences and off-cycle equilibria involved in electro-hydrogenation with complex **1** may be more complex than represented in Scheme 2, but we are confident that key aspects of the modus operandi are accurately described.

This is further reflected by kinetic studies, for which we analyzed trends of the catalytic current response with varying substrate and catalyst concentrations, to elucidate and validate details of the reaction mechanism. Specifically, in CV experiments we evaluated the catalytic peak current enhancement factors for changing concentration of 1-octene, water, or catalyst as a proxy for changing catalytic rates with changing conditions. For 1-octene, the catalytic current increases up to a concentration of approx. 60 mM, beyond which the current decreases again as a clear indication of inhibition by substrate (SI, Figure S7). This finding is in perfect agreement with our proposed alkene adduct off-cycle species. For H_2O, we found increasing catalytic current up to 1 M concentration, beyond which the current plateaus; thus, confirming that H_2O is crucial to the catalytic cycle, that it is not inhibiting the reaction, and that H_2O is not involved in the rate determining step (SI, Figure S8). For catalyst concentration (SI, Figure S9), a small but linear increase of catalytic current with increasing catalyst loading was found, probably due to mitigating inhibition by substrate at higher catalyst concentrations and further suggesting that there are no dimeric resting—or active states in the reaction cascade—as expected based on our catalytic cycle in Scheme 2.

The titration experiment confirmed the importance of H_2O for our catalytic process, nevertheless it cannot establish water as the sole source of H-atoms during electro-hydrogenation. In view of principally possible C–H activation by Ir(I) species in ($^{t\text{Bu}}$PCP)$^-$ environment, we additionally confirmed that H_2O is the actual H-donor in our electro-hydrogenation process. A bulk electrolysis control experiment in which D_2O was used instead of H_2O under otherwise analogous conditions indeed produced doubly deuterated *n*-ocatane-d_2 (SI, Section 5.5.). This finding rules out THF or Bu_4N^+ as dominant H-sources under our catalytic conditions, and further suggests that the presented electro-hydrogenation process can be used to produce partially deuterated products form D_2O as a cheap source of deuterium atoms.

Having established H_2O as the de facto source of hydrogen atoms, we performed DFT calculations to elucidate specific details of how the electro-generated anionic Ir(I)-hydride **2** reacts with H_2O, to afford the dihydride complex **3**. As relevant steps, the electro-generation of **2** and a transition state analysis of the reaction between **2** and H_2O to afford **3** were calculated (see SI, Section 8 for details). DFT calculated redox potentials for generation of **2** and electro-reduction of **3** were obtained following protocols by Grimme and co-workers,[52] allowing to benchmark the DFT results against experimental data (*c.f.* Figure 1 and SI, Figure S5), further validating the overall presented reactivity. For the electro-generation of **2** from the 16 valence electron (VE) catalyst precursor complex **1**, two successive one-electron reductions and the elimination of Cl^- are required. A key finding of the DFT study is that in order to to match the experimental reduction potential of −2.84 V for the second reduction, the intermediate formed by the first reduction cannot be the 15 VE complex [($^{t\text{Bu}}$PCP)Ir(H)] (see above).

It is therefore concluded that the coordination of L-type ligands is crucial during the electro-generation of active species **2** as reflected in Schemes 1 and 3 (see SI, Section 8 for details). The electron rich 18 VE Ir(I) complex [($^{t\text{Bu}}$PCP)Ir(H)(L)]$^-$ then liberates the L-type ligand to afford the basically equally stable 16 VE complex **2** (step **1B** to **1 C** in Scheme 3). In presence of H_2O, i.e. under electrocatalytic conditions, **2** activates water to afford Ir(III) dihydride complex **3** depicted as chemical reaction step "C" in the upper panel overview reaction of Scheme 3. A transition state analysis of the reaction revealed H_2O can be activated both, via a concerted oxidative addition pathway

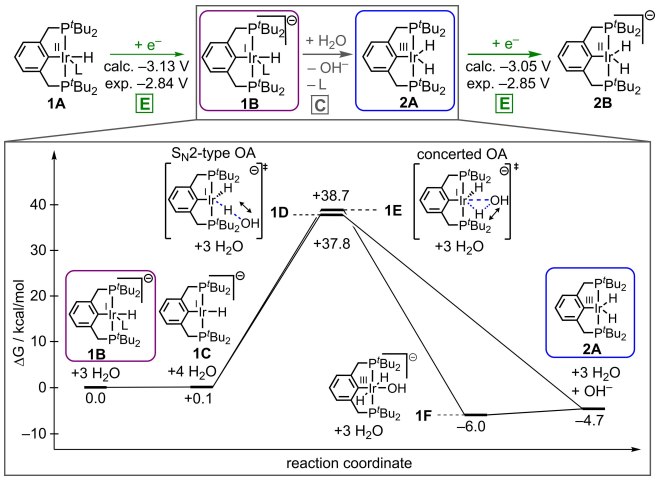

Scheme 3. DFT calculated reaction energy profile with energies given in kcal/mol and auxiliary ligand "L" referring to H_2O in the calculations.

with an activation barrier of 38.6 kcal mol^{-1}, and a S_N2-type oxidative addition with an activation barrier of 37.7 kcal mol^{-1}. The activation of water by oxidative addition distinguishes our presented electro-hydrogenation catalysis from established H^+ reduction-based examples. The product of both pathways is dihydride complex **3**, in agreement with our presented electrosynthesis of **3** from **1**; thereby, further supporting our postulated reaction mechanism (see SI, Section 8 for details). Since CV measurements of chemically synthesized complex **3** revealed a reversible reduction at −2.85 V, further validation of the calculated structure was obtained by calculating a reduction potential of −3.05 V for **3**, which is in good agreement with the experimental data.

Building on this quantum chemical insight, we desired to assess experimentally, whether the electro-hydrogenation of 1-octene with **1** is generally dependent on the H^+ activity, which should not be the case for oxidative addition of H_2O molecules.

Fundamentally, it is desirable to have processes that are robust across a range of H^+ activity and that even operate under alkaline conditions, which eliminates challenges associated with in operando changing conditions and which may boost OER at the anode at lower overpotential. To generally benchmark electro-hydrogenation with **1** for its tolerance against alkaline conditions, a controlled potential electrolysis for 1-octene hydrogenation was performed under analogous conditions to what was reported above, but with H_2O replaced by a strongly alkaline 1.0 M aqueous tetrabutylammonium hydroxide (Bu_4NOH) solution (SI, Section 5.3). After workup, *n*-octane was indeed obtained with a high FE of 89 %; thus, suggesting a high robustness of our model process against alkaline conditions.

As known from the Pourbaix diagram, H_2O oxidation is easier at high pH; thus, electro-hydrogenation with water molecules instead of H^+ paves the way to operate electrolysis at drastically reduced cell potentials, given that water oxidation potentials are reduced by ~830 mV when switching from pH = 0 to pH = 14 electrolytes.[61] Acknowledging that both necessary overpotentials of the hydrogenation half-reaction and the H_2O oxidation contribute to the cell potential, it is clear that catalyst **1** can merely serve as a model towards energy efficient ECH. For actually energy efficient processes, hydrogenation overpotentials must be drastically reduced by catalyst design in the future. In this regard, the rich literature on existing pincer- and diphosphine catalysts may serve as a pool of possible candidates, to which the herein presented reactivity can be transformed for improved energy efficiency and to circumvent the use of precious iridium in follow-up studies. Also, the electro-hydrogenation of further substrate classes with this catalyst can be developed in the future. Exemplarily, we demonstrate electro-hydrogenation of 1-octyne as a model alkyne with H_2O and catalyst **1**, for which GC-FID confirmed the formation of 1-octene with traces of *n*-octane (SI, Section 5.8).

Conclusion

In summary, the electrochemical reactivity of the Ir(III) complex [($^{t\text{Bu}}$PCP)Ir(H)(Cl)] (**1**) was investigated in THF electrolyte, which revealed the formation of anionic Ir(I) hydride complex [($^{t\text{Bu}}$PCP)Ir(H)]$^-$ (**2**) upon electrochemical reduction at −2.84 V *vs.* Fc^+/Fc. The existence of **2**, previously only postulated based on quantum chemical calculations, was now additionally confirmed by LIFDI-MS experiments with in situ reduced samples of **1**. Cyclic voltammetry experiments revealed that **2** mediates electrocatalytic hydrogenation of 1-octene as a model substrate with H_2O as the formal H-donor and electrons provided by a glassy carbon working electrode as external reducing agent. Specifics of water activation by electro-generated **2** were investigated by DFT calculations, revealing the oxidative addition of H_2O to Ir(I) as a key step. Chronoamperometry experiments confirmed a high faradaic efficiency of 96 % for the conversion of 1-octene to *n*-octane according to GC-FID, with an observed rate constant of 87 s^{-1} according to foot-of-the-wave analysis. Electrolysis with catalyst **1** and H_2O in the absence of alkene cleanly afforded Ir(III) dihydride complex [($^{t\text{Bu}}$PCP)Ir(H)$_2$] (**3**) with 88 % FE according to ^{31}P NMR. In conjunction with further control experiments showing that neither complex **1** nor complex **2** react sufficiently fast with 1-octene, **3** is proposed as the actually hydrogenating species of the electrocatalytic cycle. Finally, adding tetrabutylammonium hydroxide (Bu_4NOH) to an electrolysis sample confirmed that even under alkaline conditions catalyst **1** can efficiently hydrogenate 1-octene to *n*-octane at 89 % FE. Accordingly, the herein presented electro-hydrogenation activity does not critically rely on the activity of free protons, which makes the process robust and allows to adjust proton activity with respect to requirements at the counter electrode. For a future perspective of further developing the electro-hydrogenation reactivity of **1** with water, we exemplify the electrodeuteration of 1-octene with D_2O to *n*-octane-d_2 and the electro-hydrogenation of 1-octyne.

Acknowledgements

D.H. thanks the Fonds der Chemischen Industrie for a Liebig Fellowship. This work was further supported by a Feodor Lynen Return Fellowship for D.H. by the Alexander von Humboldt Foundation and the TUM Junior Fellow Funds by the Technical University of Munich. P.M., M.D., A.F. and D.H. are grateful for support by Roland A. Fischer and his chair of Inorganic and Metal-Organic Chemistry at TUM. Open Access funding enabled and organized by Projekt DEAL.

Conflict of Interest

The authors declare no conflict of interest.

Data Availability Statement

The data that support the findings of this study are available from the corresponding author upon reasonable request.

Keywords: Ir(III)-pincer · electrochemical hydrogenation · cyclic voltammetry · anionic Ir(I) hydride · electro-synthesis

[1] L. Alig, M. Fritz, S. Schneider, *Chem. Rev.* **2019**, *119*, 2681.
[2] M. A. Stoffels, F. J. R. Klauck, T. Hamadi, F. Glorius, J. Leker, *Adv. Synth. Catal.* **2020**, *362*, 1258.
[3] H.-U. Blaser, C. Malan, B. Pugin, F. Spindler, H. Steiner, M. Studer, *Adv. Synth. Catal.* **2003**, *345*, 103.
[4] H. Jorschick, M. Vogl, P. Preuster, A. Bösmann, P. Wasserscheid, *Int. J. Hydrogen Energy* **2019**, *44*, 31172.
[5] Y. Nakagawa, M. Tamura, K. Tomishige, *ACS Catal.* **2013**, *3*, 2655.
[6] S. Werkmeister, J. Neumann, K. Junge, M. Beller, *Chem. Eur. J.* **2015**, *21*, 12226.
[7] J. G. D. Vries, C. J. Elsevier (Eds.) *The handbook of homogeneous hydrogenation*, Wiley-VCH, Weinheim, **2007**.
[8] D. Wang, D. Astruc, *Chem. Rev.* **2015**, *115*, 6621.
[9] R. Nie, Y. Tao, Y. Nie, T. Lu, J. Wang, Y. Zhang, X. Lu, C. C. Xu, *ACS Catal.* **2021**, *11*, 1071.
[10] X. Hu, G. Wang, C. Qin, X. Xie, C. Zhang, W. Xu, Y. Liu, *Org. Chem. Front.* **2019**, *6*, 2619.
[11] Y. Gao, X. Zhang, R. D. Laishram, J. Chen, K. Li, K. Zhang, G. Zeng, B. Fan, *Adv. Synth. Catal.* **2019**, *361*, 3991.
[12] K. Li, R. Khan, X. Zhang, Y. Gao, Y. Zhou, H. Tan, J. Chen, B. Fan, *Chem. Commun.* **2019**, *55*, 5663.
[13] S. Guo, X. Wang, J. S. Zhou, *Org. Lett.* **2020**, *22*, 1204.
[14] S. Rao, K. R. Prabhu, *Chem. Eur. J.* **2018**, *24*, 13954.
[15] Q. Xuan, Q. Song, *Org. Lett.* **2016**, *18*, 4250.
[16] J. Derosa, P. Garrido-Barros, J. C. Peters, *J. Am. Chem. Soc.* **2021**, *143*, 9303.
[17] J. Li, L. He, X. Liu, X. Cheng, G. Li, *Angew. Chem. Int. Ed.* **2019**, *58*, 1759.
[18] J. Bu, Z. Liu, W. Ma, L. Zhang, T. Wang, H. Zhang, Q. Zhang, X. Feng, J. Zhang, *Nat. Catal.* **2021**, *4*, 557.
[19] B. Li, H. Ge, *Sci. Adv.* **2019**, *5*, eaaw2774.
[20] B.-H. Zhao, F. Chen, M. Wang, C. Cheng, Y. Wu, C. Liu, Y. Yu, B. Zhang, *Nat Sustain* **2023**, *6*, 827.
[21] S. H. Langer, S. Yurchak, *J. Electrochem. Soc.* **1969**, *116*, 1228.
[22] Y. Inami, H. Ogihara, S. Nagamatsu, K. Asakura, I. Yamanaka, *ACS Catal.* **2019**, *9*, 2448.
[23] N. Itoh, W. Xu, S. Hara, K. Sakaki, *Catal. Today* **2000**, *56*, 307.
[24] B. K. Peters, K. X. Rodriguez, S. H. Reisberg, S. B. Beil, D. P. Hickey, Y. Kawamata, M. Collins, J. Starr, L. Chen, S. Udyavara, K. Klunder, T. J. Gorey, S. L. Anderson, M. Neurock, S. D. Minteer, P. S. Baran, *Science* **2019**, *363*, 838.
[25] I. Fokin, I. Siewert, *Chem. Eur. J.* **2020**, *26*, 14137.
[26] M. J. Chalkley, P. Garrido-Barros, J. C. Peters, *Science* **2020**, *369*, 850.
[27] I. Fokin, K.-T. Kuessner, I. Siewert, *ACS Catal.* **2022**, *12*, 8632.
[28] C. H. Lam, C. B. Lowe, Z. Li, K. N. Longe, J. T. Rayburn, M. A. Caldwell, C. E. Houdek, J. B. Maguire, C. M. Saffron, D. J. Miller, J. E. Jackson, *Green Chem.* **2015**, *17*, 601.
[29] S. Kim, E. E. Kwon, Y. T. Kim, S. Jung, H. J. Kim, G. W. Huber, J. Lee, *Green Chem.* **2019**, *21*, 3715.
[30] W. Liu, W. You, Y. Gong, Y. Deng, *Energy Environ. Sci.* **2020**, *13*, 917.
[31] A. Kurimoto, R. S. Sherbo, Y. Cao, N. W. X. Loo, C. P. Berlinguette, *Nat. Catal.* **2020**, *3*, 719.
[32] J. Yang, H. Qin, K. Yan, X. Cheng, J. Wen, *Adv. Synth. Catal.* **2021**, *363*, 5407.
[33] R. S. Sherbo, R. S. Delima, V. A. Chiykowski, B. P. MacLeod, C. P. Berlinguette, *Nat. Catal.* **2018**, *1*, 501.
[34] P. Garrido-Barros, J. Derosa, M. J. Chalkley, J. C. Peters, *Nature* **2022**, *609*, 71.
[35] J. Derosa, P. Garrido-Barros, M. Li, J. C. Peters, *J. Am. Chem. Soc.* **2022**, *144*, 20118.
[36] S. A. Akhade, N. Singh, O. Y. Gutiérrez, J. Lopez-Ruiz, H. Wang, J. D. Holladay, Y. Liu, A. Karkamkar, R. S. Weber, A. B. Padmaperuma, et al., V.-A. Glezakou, *Chem. Rev.* **2020**, *120*, 11370.
[37] M. Wakisaka, M. Kunitake, *Electrochem. Commun.* **2016**, *64*, 5.
[38] H. Carrero, J. Gao, J. F. Rusling, C.-W. Lee, A. J. Fry, *Electrochim. Acta* **1999**, *45*, 503.
[39] P. Li, R. Zhao, H. Chen, H. Wang, P. Wei, H. Huang, Q. Liu, T. Li, X. Shi, Y. Zhang, M. Liu, X. Sun, *Small* **2019**, *15*, 1805103.
[40] O. V. Ozerov, *Chem. Soc. Rev.* **2009**, *38*, 83.
[41] D. Morales-Morales, D. W. Lee, Z. Wang, C. M. Jensen, *Organometallics* **2001**, *20*, 1144.
[42] C. Liu, Y. Wu, B. Zhao, B. Zhang, *Acc. Chem. Res.* **2023**, *56*, 1872.
[43] Y. Wu, C. Liu, C. Wang, S. Lu, B. Zhang, *Angew. Chem. Int. Ed.* **2020**, *59*, 21170.
[44] J. Sheng, X. Cheng, *CCS Chem* **2024**, *6*, 230.
[45] C. J. Moulton, B. L. Shaw, *J. Chem. Soc. Dalton Trans.* **1976**, 1020.
[46] M. Rimoldi, A. Mezzetti, *Inorg. Chem.* **2014**, *53*, 11974.
[47] T. Abura, S. Ogo, Y. Watanabe, S. Fukuzumi, *J. Am. Chem. Soc.* **2003**, *125*, 4149.
[48] S. I. Johnson, R. J. Nielsen, W. A. Goddard, *ACS Catal.* **2016**, *6*, 6362.
[49] D. Y. Wang, Y. Choliy, M. C. Haibach, J. F. Hartwig, K. Krogh-Jespersen, A. S. Goldman, *J. Am. Chem. Soc.* **2016**, *138*, 149.
[50] I. Osadchuk, T. Tamm, M. S. G. Ahlquist, *ACS Catal.* **2016**, *6*, 3834.
[51] P. Kang, C. Cheng, Z. Chen, C. K. Schauer, T. J. Meyer, M. Brookhart, *J. Am. Chem. Soc.* **2012**, *134*, 5500.
[52] H. Neugebauer, F. Bohle, M. Bursch, A. Hansen, S. Grimme, *J. Phys. Chem. A* **2020**, *124*, 7166.
[53] J. L. Dye, *Science* **1990**, *247*, 663.
[54] L. Cao, C. Sun, N. Sun, L. Meng, D. Chen, *Dalton Trans.* **2013**, *42*, 5755.

[55] C. Sandford, M. A. Edwards, K. J. Klunder, D. P. Hickey, M. Li, K. Barman, M. S. Sigman, H. S. White, S. D. Minteer, *Chem. Sci.* **2019**, *10*, 6404.
[56] M. Kanzelberger, X. Zhang, T. J. Emge, A. S. Goldman, J. Zhao, C. Incarvito, J. F. Hartwig, *J. Am. Chem. Soc.* **2003**, *125*, 13644.
[57] A. Kumar, T. Zhou, T. J. Emge, O. Mironov, R. J. Saxton, K. Krogh-Jespersen, A. S. Goldman, *J. Am. Chem. Soc.* **2015**, *137*, 9894.
[58] K. Krogh-Jespersen, M. Czerw, A. S. Goldman, in ACS Symposium Series, *Vol. 885* (Eds.: K. Krogh-Jespersen, M. Czerw, A. S. Goldman), American Chemical Society, Washington, DC, **2004**, pp. 216–233.
[59] A. B. P. Lever, *Inorg. Chem.* **1990**, *29*, 1271.
[60] M. Wilklow-Marnell, B. Li, T. Zhou, K. Krogh-Jespersen, W. W. Brennessel, T. J. Emge, A. S. Goldman, W. D. Jones, *J. Am. Chem. Soc.* **2017**, *139*, 8977.
[61] M. W. Kanan, D. G. Nocera, *Science* **2008**, *321*, 1072.

Manuscript received: November 22, 2023
Accepted manuscript online: May 17, 2024
Version of record online: July 1, 2024